

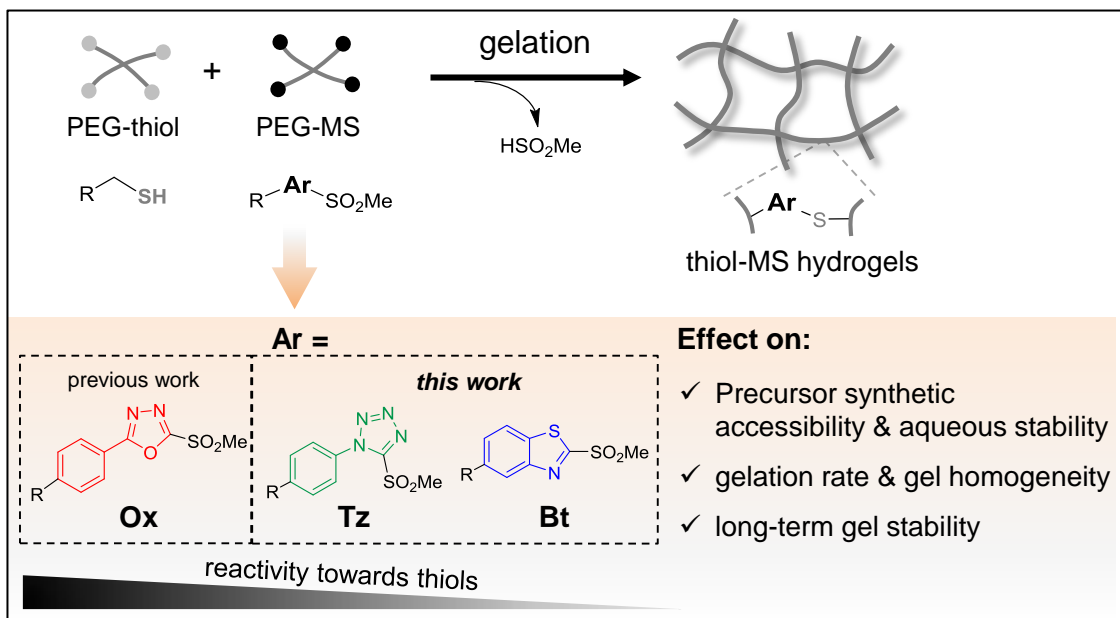
Thiol-methylsulfone-based hydrogels for cell encapsulation: reactivity optimization of aryl-methylsulfone substrate for fine-tunable gelation rate and improved stability

Julieta I. Paez,^{*†} Adrián de Miguel-Jiménez,^{†‡} Rocío Valbuena-Mendoza,^{†‡} Aditi Rathore,[†] Minye Jin,^{†‡} Alisa Gläser,[†] Samuel Pearson[†] and Aránzazu del Campo^{*†‡}

[†] INM – Leibniz Institute for New Materials, Campus D2-2, 66123, Saarbrücken, Germany.

[‡] Saarland University, Chemistry Department, 66123 Saarbrücken, Germany.

Corresponding authors: julieta.paez@leibniz-inm.de; aranzazu.delcampo@leibniz-inm.de



KEYWORDS: thiol-arylmethylsulfone, cell encapsulation, PEG hydrogels, water-based crosslinking reactions, gel stability, gelation kinetics

ABSTRACT:

Hydrogels are widely used as hydrated matrices for cell encapsulation in a number of applications, spanning from advanced 3D cultures and tissue models to cell-based therapeutics and tissue engineering. Hydrogel formation in the presence of living cells requires crosslinking reactions that proceed efficiently under close to physiological conditions. Recently, the nucleophilic aromatic substitution of phenyl-oxadiazole (Ox) methylsulfones (MS) by thiols was introduced as a new crosslinking reaction for cell encapsulation. Reported poly(ethylene glycol) (PEG)-based hydrogels featured tunable gelation times within seconds to a few minutes within pH 8.0 to 6.6 and allowed reasonably good mixing with cells. However, their rapid degradation prevented cell cultures to be maintained beyond 1 week. In this article, we present the reactivity optimization of the heteroaromatic ring of the MS partner to slow down the crosslinking kinetics and the degradability of derived hydrogels. New MS substrates based on phenyl-tetrazole (Tz) and benzothiazole (Bt) rings, with lower electrophilicity than Ox, were synthesized by simple pathways. When mixed with PEG-thiol, the novel PEG-MS extended the working time of precursor mixtures and allowed longer term cell culture. Tz-based MS substrate was identified as the best candidate as it is accessible by simple chemical reactions from cost-effective reactants, hydrogel precursors show > 3 months stability in aqueous solution, and the derived Tz gels support cell cultures for > 2 weeks. The Tz system also shows tunable gelation kinetics within seconds to hours and allows comfortable manipulation and cell encapsulation. Our findings expand the toolkit of thiol-mediated chemistry for the synthesis of hydrogels with improved properties for laboratory handling and future automatization.

1. Introduction

Cell-encapsulating hydrogels are used as supportive microenvironments in cell biology and biomedical applications. These materials can be synthesized with defined molecular architectures, mechanical properties and biochemical cues tailored to the needs of different cell types. Their application potential is broad, spanning from in vitro models for cell culture and drug testing, to injectable matrices for cell therapies or regenerative medicine.¹

The crosslinking reaction to form the hydrogel network from polymer precursor needs to be carried out in the presence of cells. Therefore, it has to show high efficiency under physiological conditions and occur at an adequate rate to yield hydrogel-cell constructs with homogeneous distribution of the embedded cells. Systems with reaction rates that are tunable by small changes in pH, temperature, or buffer concentration are particularly interesting because they can be adapted to facilitate handling in different processing scenarios. Ideally, the crosslinking reaction should also be bioorthogonal, render stable bonds in physiological milieu and use cost-effective precursors. The most popular covalent crosslinking strategies are radical-mediated acrylic² and thiol-ene³ polymerizations, Schiff-base formation,⁴ cycloadditions⁵, and thiol-mediated Michael-type additions, which exhibit some but not all of these desirable features.⁶ Developing a crosslinking platform that brings all the favorable characteristics together remains a challenge and motivates researchers to expand the present chemical toolkit.

Recently, our group introduced the thiol-methylsulfonyl-based reaction as a covalent and cytocompatible crosslinking strategy for cell encapsulation.⁷ It is based on the nucleophilic aromatic substitution of aryl-methylsulfones (MS) by thiols to yield aryl-thioether adducts, with the release of a methylsulfonate anion as leaving group. In this system, where aryl = phenyl-

oxadiazole (Ox), hydrogels featured gelation times in the range of seconds to minutes. This gelation rate allowed complete mixing of polymeric precursors and cell suspensions under low shear forces on a convenient timescale, and led to hydrogels with a homogeneous distribution of embedded cells. Furthermore, the gelation rate of Ox-based thiol-MS gels could be precisely regulated by adjusting the pH from 8.0 to 6.6 to achieve gelation times between a few seconds and a couple of minutes. Despite these important advantages, the reported thiol-Ox-MS gels presented some limitations: relatively low stability of precursors under storage, relatively fast degradation rate (lasting < 1 week) in cell culture conditions, and expensive reactants. In addition, we realized that an extension of the gelation time window would also be beneficial from an application perspective, in order to facilitate longer mixing time and handling of the precursor mixtures.

From a molecular point of view, a lower electrophilicity of the MS ring is expected to slow down the reaction rate⁸ with thiols, and lead to more stable aryl-thioether adducts.^{8a} In this work, we explore MS substrates based on phenyl-tetrazole (Tz) and benzothiazole (Bt) heteroaryl rings linked to PEG backbones (**Figure 1A**) to investigate the structure-reactivity relationship that leads to materials with improved properties. We identified the Tz MS substrate as a particularly interesting system for cell encapsulation. Tz-based MS precursors are (i) accessible from cost-effective reactants and simple reaction steps, and (ii) present high stability for storage in aqueous solution (> 3 months). Derived Tz-based thiol-MS gels demonstrate lower degradation rate than Ox analogues and support cell culture for > 2 weeks. At the same time, the Tz system shows tunable gelation kinetics within seconds to hours and allows comfortable manipulation and cell encapsulation. Our findings expand the toolkit of thiol-mediated chemistry for the synthesis of hydrogels with tailorable properties to be used in pharmacy and medicine.

2. Results and Discussion

Synthesis of Tz and Bt-based PEG-MS precursors and stability study in aqueous solution

One possibility to reduce the rate of the thiol-MS reaction is to use heteroaryls with lower electron-withdrawing character.⁹ For utility in cell encapsulation, water solubility, stability in solution of the aryl-thioether adduct, or low price of precursors should not be compromised. Based on these prerequisites and reported reactivity studies of thiol-MS systems,^{8a, 9b} we selected the MS heterocycles 5-(methylsulfonyl)-1-phenyl-1H-tetrazole (Tz) and 2-(methylsulfonyl)-1,3-benzothiazole (Bt) (see structures in Figure 1A) as candidates to compare with our existing Ox system. These heterocycles show decreasing electron-withdrawing character in the order Ox > Tz > Bt and, consequently, the second-order reaction rate constant for coupling with thiols under aqueous conditions (in buffer at pH 7.5) decreases from 450 (Ox) to 6-17 (Tz) to 0.3-0.5 (Bt) M⁻¹s⁻¹.^{8b, 9b} Note that these rate constants match well with those of common coupling reactions employed for crosslinking of cell-encapsulating gels, which typically exhibit second-order rate constant $\sim 10^{-1}$ to 10^2 M⁻¹s⁻¹ in aqueous buffer at pH 7.4.⁷ In addition, the Tz and Bt substrates can be prepared with reasonable synthetic effort from inexpensive precursors (2 and 30 € per gram, respectively), and feature good water solubility; thus representing a significant cost advantage that will facilitate economical upscaling. For comparison, the Ox precursor costs 1,000 € per gram.

Starting from the commercial Tz and Bt precursors, 4-arm star PEG-Bt and PEG-Tz macromers (molar mass 20 kDa) were synthesized in 5-6 steps (see Supporting Information). The synthesis of PEG-Bt started from 5-methoxy-1,3-benzothiazole-2-thiol via cleavage of the methoxy ether using aluminum(III) chloride to obtain the free phenol, followed by selective

methylation of the thiol group with methyl iodide. After etherification of the phenol with 2-(Boc-amino)ethyl bromide, oxidation of the methylthioether moiety to methylsulfone was performed, followed by Boc cleavage. A final coupling of the free amine to PEG-NHS afforded the PEG-Bt macromer. PEG-Tz was synthesized in a similar manner starting from 4-(5-thiol-1H-tetrazol-1-yl)phenol, therefore not requiring the demethoxylation step. PEG-Bt and PEG-Tz macromers were obtained in high purity and with yields >80% after purification by dialysis. The polymers showed a substitution degree >90%. PEG-Ox macromer was synthesized in 3 steps as previously reported.⁷ All the PEG-MS compounds remained stable as solids stored at -20°C for > 6 months. Further details on the synthesis and characterization of intermediates and final macromers are included in the Supporting Information (SI).

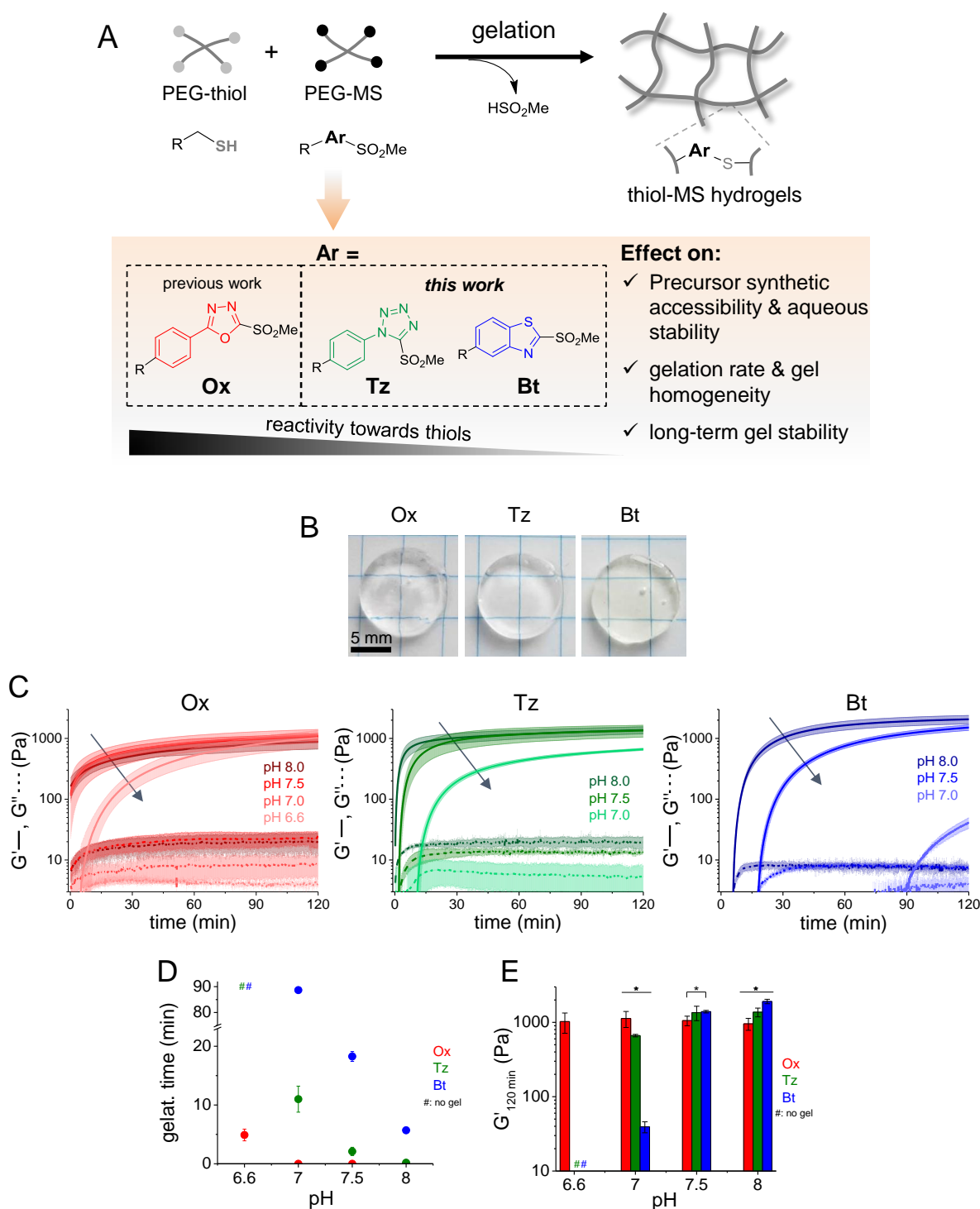


Figure 1. Comparison of rheological properties of PEG-based thiol-MS hydrogels. **A)** Schematics of thiol-MS crosslinking and chemical structures of the MS heteroaryl substrates used in this work. **B)** Images of swollen PEG thiol-MS gels. **C)** Rheological curves showing the shear storage (G') and loss (G'') moduli as a function of time and pH during gel formation for the different hydrogel compositions. The arrows indicate the direction of pH decrease. **D)** Gelation

time and **E**) $G'_{120 \text{ min}}$ (before swelling) from the rheology curves in C). Gelation conditions: 5 wt% polymer, 10 mM HEPES, 25°C. Data are mean \pm SD (n= 3); in E) *p < 0.05, one-way ANOVA with Tukey post-hoc test. In D-E), # indicates that no gel was formed under that specific condition.

The stability of the different PEG-MS macromers in water at ambient conditions (room temperature, normal light exposure) was investigated by ^1H NMR spectroscopy for 12 weeks (Figure S1). PEG-Tz remained stable for >12 weeks. PEG-Bt and PEG-Ox degraded after 3 weeks and 1 week of storage, respectively, as evidenced by spectral changes in the aromatic region (Figure S1). The degradation rate observed for PEG-Ox is in good agreement with a recent study of the Ox small molecule,^{9b} while the superior stability of the Tz substrate vs. Bt is a new finding from this work. Interestingly, the stability trend $\text{Tz} \gg \text{Bt} > \text{Ox}$ does not correlate with the decreasing electrophilicity of the MS ring ($\text{Ox} > \text{Tz} > \text{Bt}$), suggesting that the stability profile might be influenced by other factors such as water solubility, polarity, and steric hindrance.

Effect of MS electrophilicity on gelation rate, crosslinking degree and stability profile under physiological conditions

The gelation reaction was studied in 10 mM HEPES buffer at pH 8.0 and 25°C. PEG-MS and PEG-thiol solutions at 5 wt% were mixed in equivolumes and at a 1:1 thiol:MS molar ratio, forming hydrogels that appeared transparent and homogeneous to the naked eye (see representative pictures in Figure 1B). From this point onwards, we refer to the different thiol-MS gels by the type of MS precursor (i.e. Ox, Tz, and Bt gels). Under the specified preparation conditions, gelation time points (as measured in a microscopic pipetting test⁷) were 3 s, 36 s and 4.6 min for Ox, Tz and Bt variants, respectively (**Table 1**). These results reflect a decreasing

reactivity of the heteroaryl MS in the order Ox > Tz > Bt, and validate our hypothesis for the molecular design. By modulating the pH between 8.0 and 6.6, gelation times could be adjusted within a very broad range: seconds to minutes for Ox, seconds to hours for Tz, and minutes to hours for Bt (Table 1).

Table 1. Gelation time points of the different thiol-MS hydrogels at 5 wt% concentration and at varying pH values, as measured by a macroscopic pipetting test.

gel	pH			
	6.6	7.0	7.5	8.0
Ox ^(a)	4 min	12 s	6 s	3 s
Tz	1.9 h	7.1 min	1.7 min	36 s
Bt	3.2 h	23.2 min	9.2 min	4.6 min

^(a)Values taken from our previous work.⁷ Measurement conditions: 5 wt% polymer concentration, in 10 mM HEPES buffer, 25°C; in pH range from 6.6 to 8.0.

Oscillatory rheology experiments corroborated the macroscopic gelation observations. The PEG-MS and PEG-thiol solutions were mixed directly on the rheometer plate, and the evolution of shear storage (G') and loss (G'') moduli during crosslinking at 25°C was monitored. The gelation time point, defined at the crossover point of G' and G'' in the time sweep curves, followed the order Ox < Tz < Bt (Figure 1D) and also increased with decreasing pH of the solution. In the pH range from 8.0 to 7.0, Ox hydrogels showed a gelation time < 1 min, whereas Tz hydrogels took from < 1 min to 11 min and Bt formed hydrogels from 6 min to 1.5 hours (Figure 1D). At pH 6.6, gelation time of Ox increased to 5 min, whereas Tz and Bt did not gel within 2 h. These results confirm that different MS heteroaryl units can form hydrogels within a

few seconds to hours by varying the pH within the physiological range 8.0 to 6.6. In particular, the possibility to tune gelation kinetics between seconds to several minutes is advantageous in many scenarios, for example in the development of injectable matrices that provide sufficient time to administer the gel at the desired location in the body while avoiding premature gelation inside the syringe.¹⁰ According to our previous results, the gelation rate of thiol-MS hydrogels is intermediate between gelation rate of the thiol-Mal and the thiol-VS systems (i.e. thiol-Mal > Ox > Tz > Bt > thiol-VS).⁷

The influence of the pH on the extent of the crosslinking reaction and, consequently, on the mechanical stability of the crosslinked hydrogel was examined (Figure 1E and Figure S2A). Ox gels prepared from pH 8.0 to 7.0 showed similar $G'_{120 \text{ min}}$ values ranging from 960 to 1130 Pa.⁷ In contrast, Tz and Bt formed hydrogels with much greater variability in G' across this pH range. Tz gels showed consistent $G'_{120 \text{ min}} \sim 1360$ Pa at pH values of 8.0 and 7.5, but significantly lower $G'_{120 \text{ min}}$ at pH 7.0 (~ 660 Pa). Bt gels showed decreasing G' value with decreasing pH ($G'_{120 \text{ min}} \sim 1900, 1400$ and 40 Pa at pH 8.0, 7.5 and 7.0, respectively) (Fig. S2A). Note that at pH 7.0, G' values had not plateaued by 120 min, and the observed decrease in $G'_{120 \text{ min}}$, Ox > Tz > Bt, therefore reflects the degree to which the crosslinking had progressed in accordance with the order of MS substrate reactivity. At pH 8.0, all gels did reach a plateau in G' , and the reverse trend in $G'_{120 \text{ min}}$ was found: Bt > Tz > Ox, presumably because a slower crosslinking rate renders a network with fewer defects and higher crosslinking.⁷ Altogether, our results reveal that the combination of MS reactivity and pH allows adjusting of gelation rate and crosslinking degree of the final hydrogel.

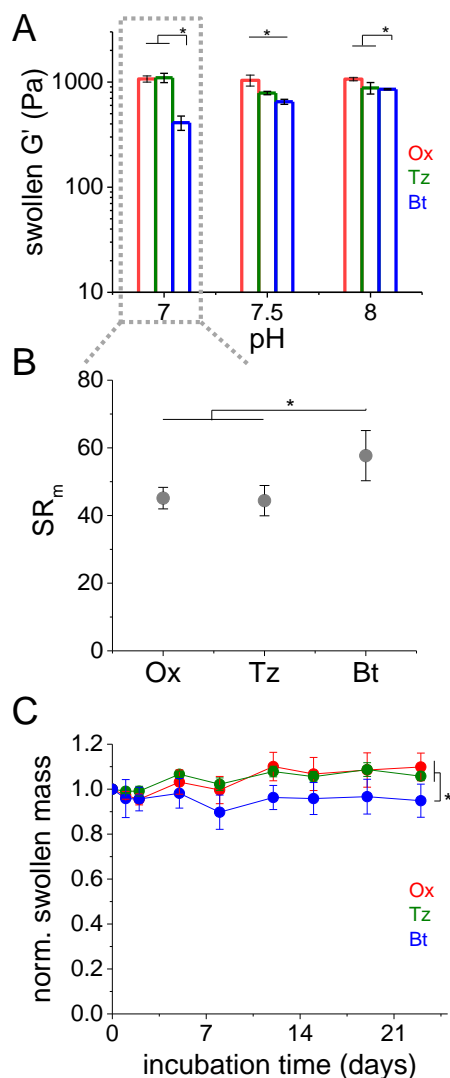


Figure 2. Mechanical, swelling, and stability properties of different thiol-MS hydrogels. **A)** $G'_{120\text{ min}}$ after swelling at increasing pH from 7.0 to 8.0. **B)** Mass swelling ratio in water, pH 7.0. **C)** Stability study of gels upon incubation in cell culture medium over 3 weeks (RPMI+, pH 7.4, 37°C), followed as the mass of swollen gel as a function of incubation time. Conditions: 5 wt% polymer, 10 mM HEPES, cured for 120 min, 25°C. Data are mean \pm SD ($n=3$); * $p < 0.05$, one-way ANOVA with Tukey post-hoc test.

The mechanical properties of thiol-MS gels after swelling in buffer for 24 h were also studied. (Figure 2A and Figure S2B). G' values of swollen Ox samples obtained at different pH were similar ($G' \sim 1050$ Pa), while Bt gels obtained at pH between 7.0 and 8.0 showed increasing post-swelling G' values (from 410 to 860 Pa). These trends are similar to those observed before

swelling (Fig. 1E). This was in contrast to swollen Tz gels, which showed a G' of 1100, 790 and 880 Pa when gelation was performed at pH 7.0, 7.5 or 8.0. Surprisingly, this trend was contrary to that observed before swelling (Fig. 1E). The reason for this difference is unclear at the moment.

The mass swelling ratio (SR_m) of the thiol-MS gels prepared at pH 7.0 was 1.3-fold higher for Bt gel (58 ± 7) than for the other two systems (44 ± 4 for Tz and 45 ± 3 for Ox) (Fig. 2B). This suggests that Bt hydrogels have a lower crosslinking density, in good agreement with the ~ 2.6 -fold lower value of G' observed in the swollen samples (swollen $G' = 410 \pm 64$ Pa for Bt vs. 1100 ± 110 Pa for Tz and 1070 ± 73 Pa for Ox, Fig. 2A).

The gels' stabilities in serum-containing RPMI cell culture medium (pH 7.4) at 37°C was tested (Figure 2C). Ox and Tz gels showed a mass increase (i.e. water uptake) of 10 and 6%, respectively at day 23, whereas Bt gels showed a mass loss of 5%. These results suggest that all thiol-MS gels are stable over the course of the study. A deeper analysis of gel stability under cell culture conditions is presented later in this work.

Modulation of pH value and buffer concentration enable fine-tuning of gelation rate for Tz gels

The thiol-MS coupling is expected to proceed through the addition of the thiolate anion at the substituted position of the heteroaromatic MS electrophile to form a negatively charged intermediate (called σ -complex), with subsequent release of a methanesulfinat anion as leaving group.¹¹ Because this reaction involves polar species, its rate in aqueous media could be affected by changes in buffer concentration, possibly due to solvation effects of the reactive pair and of the σ -complex intermediate.¹² Indeed, recent reports on thiol-MS coupling applied to

bioconjugation have demonstrated that the increase of PBS buffer concentration from 1 to 50 mM resulted in 4-fold higher reaction conversions after a fixed reaction time (pH 7.4, room temperature, 30 min).^{8a} Based on these observations, we tested whether buffer concentration can regulate gelation kinetics in the thiol-MS gel system. Experiments were performed with Tz gels because their gelation rate enables comfortable sample preparation in the rheometer. To better visualize the modulatory effect of both buffer concentration and pH value for on-demand regulation of gelation kinetics, a stepwise gelation program was tested and monitored in the rheometer. Tz gels at 5 wt% concentration were prepared in 10 mM HEPES and pH 7.0. Under these conditions, the gelation point is achieved at 11 min, the crosslinking process of the gel takes > 2 h to achieve a plateaued G' , and $G'_{120 \text{ min}} \sim 660 \text{ Pa}$ (see Fig. 1C-D and **Figure 3A**). At $t = 20 \text{ min}$, when a soft but stable gel was formed ($G' \sim 85 \text{ Pa}$), buffer of increasing concentration (10, 20 or 50 mM) and pH (7.0 or 8.0) was added to the lower rheometer plate in separate experiments. When fresh buffer with the same composition as the initial one was added (10 mM HEPES, pH 7.0), a noticeable change in the gelation curve was observed, characterized by a steeper increase of G' and a higher $G'_{120 \text{ min}} = 2625 \text{ Pa}$ at the end of the experiment (Fig. 3A and **Table 2**) versus the control experiment in which no new buffer was added. We speculate this effect is due to swelling of the network under geometrical constraints (since the curing sample is located between the rheometer plates), which is accompanied by increased mobility of pendant reactive groups that rapidly couple complementary partners thus leading to higher G' (i.e. increased conversion). In line with results from Fig. 1C, pH increase of 10 mM buffer from 7.0 to 8.0 accelerated the gelation rate, while attaining a similar $G'_{120 \text{ min}}$ (2625 and 2974 Pa, respectively). Furthermore, increase of buffer concentration from 10 to 50 mM at constant pH 8.0 resulted in acceleration of the gelation rate, in good agreement with previous reports on thiol-

MS coupling on small molecules.^{8a} Increasing buffer concentration also produced a higher G' at the end of the experiment (from 2974 to 3755 Pa). This could be due to a higher crosslinking degree; however some small differences in the swelling of the neutral PEG chains at varying ionic strength might also occur.¹³

To better illustrate the dependence of gelation rate on buffer concentration and pH, the gelation rate at the different conditions was extracted from the rheology curves by fitting them to an exponential growth equation (Fig. 3B and **Table 2**). An increase in buffer concentration from 10 to 50 mM (pH 8.0) doubled the observed gelation rate constant k_{obs} . A combined increase of pH from 7.0 to 8.0 and of buffer concentration from 10 to 50 mM led to a 5-fold increase in the gelation rate. A fine-tunable kinetics of the gelation process is advantageous for the combination of the cell encapsulation steps with scaffold processing technologies, such as 3D bioprinting, where processing and stabilization of the printed structures is often performed with stepwise crosslinking.¹⁴

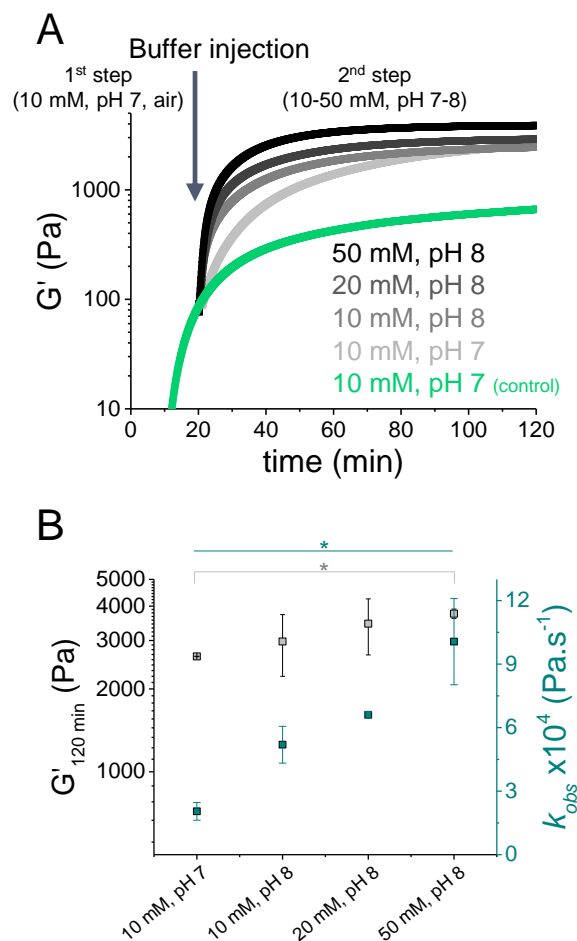


Figure 3. Modulation of gelation rate of Tz gels by pH and buffer concentration. **A)** Representative time sweep curves showing G' during stepwise gelation. The curing sample (in 10 mM HEPES, pH 7) was set on the rheometer plate and allowed to cure in air for 20 min. Subsequently, buffer of given pH (7.0-8.0) and concentration (10-50 mM) was injected to the rheometer's lower plate (indicated by the arrow) and the gelation continued from 20 to 120 min. **B)** Shear storage modulus and gelation kinetics, corresponding to the second curing step shown in A), $G'_{120 \text{ min}}$ and estimated gelation rate constant are reported. Conditions: 5 wt% polymer, HEPES, 25°C. In B), data are mean \pm SD ($n = 2$); * $p < 0.05$, one-way ANOVA with Tukey post-hoc test.

Table 2. Mechanical and kinetic properties of Tz-based thiol-MS gels during a two-step gelation program with pH and buffer concentration modulation, as measured by in situ rheology.

entry	gelation conditions		gel properties		
	1 st step	2 nd step	mechanics	gelation rate of 2 nd step	
			$G'_{120 \text{ min}}$ (Pa)	$k_{obs} \times 10^4$ (Pa s ⁻¹)	k_{obs} (relat.)
1		10 mM, pH 7.0	2625	2.05 ± 0.42	1.0
2	10 mM, pH 7	10 mM, pH 8.0	2974	5.2 ± 0.9	2.5
3		20 mM, pH 8.0	3453	6.6 ± 0.1	3.2
4		50 mM, pH 8.0	3755	10.1 ± 2.0	4.9

Measurement conditions: 5 wt% polymer concentration, in HEPES buffer (10, 20 or 50 mM concentration), at variable pH (7.0 or 8.0), 25°C.

MS substrate reactivity influences microscale homogeneity of gels

The rate of the crosslinking reaction in a two-component reactive gel mixture influences the homogeneity of the precursors mixture and, consequently, the microscale homogeneity of the resulting hydrogel.¹⁵ Gel inhomogeneity has been demonstrated to compromise the reproducibility and outcome of cell cultures.¹⁵⁻¹⁶ We examined the microscale homogeneity of the thiol-MS hydrogels using fluorescently labelled PEG-thiol precursors (see details in Exp. Section). Hydrogels were prepared at 5 wt% concentration and at pH 8.0, which are representative conditions used for cell encapsulation (i.e within the typical range of 4-10 wt% concentration and pH 7.4 to 8.0).^{6a, 7, 17} Under our tested conditions, gelation time points vary from 3 s (Ox), to 36 s (Tz) to 4.6 min (Bt). This allows Tz and Bt gel precursors to be better mixed before noticeable increase of viscosity occurs in the mixture, while Ox gel precursors provide a shorter time window for mixing. To reveal the microscale homogeneity of the hydrogels, a fluorophore was covalently coupled to the hydrogel and the fluorescence intensity

across the sample was imaged by confocal microscopy (**Figure 4A**). Fast-crosslinking Ox gels showed an inhomogeneous fluorescence distribution, in contrast to Tz and Bt gels. Gelation time points > 30 s rendered more homogeneous hydrogels, in good agreement with previous reports on thiol-VS hydrogels (gelation time point = 8 min under same conditions).⁷ This is a relevant point for the transfer of encapsulating systems to automatized cell culture and standardized cell assays.^{1b, 18}

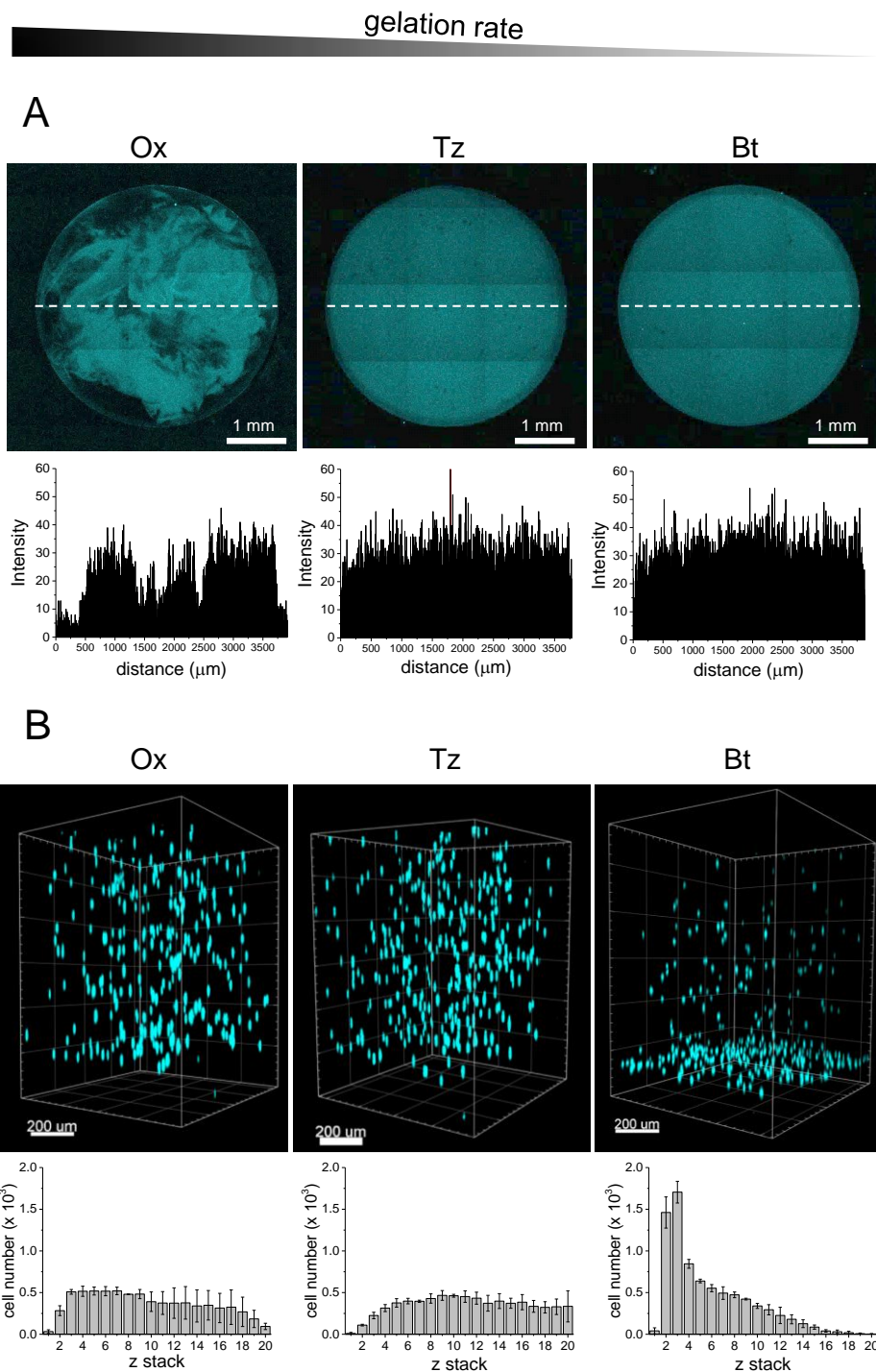


Figure 4. Effect of gelation rate on the microscale homogeneity of diverse thiol-MS gels by fluorescence confocal microscopy. **A)** Image of fluorescently labeled gels and fluorescence intensity distribution as a function of distance across the gel, following the region of interest indicated by the white line, scale bar = 1 mm. Gel composition: 5 wt% polymer, 0.01 mM Alexa-Fluor 350-maleimide, 20 mM HEPES pH 8.0. **B)** Analysis of density distribution of encapsulated

cells (L929 fibroblasts) across the gels, showing images and cell number distribution over z-stacks (scale bar = 200 μm , z-stack step = 50 μm), after 1 h post-encapsulation and DAPI staining (cyan) of cell nuclei. Gel composition: 4 wt% polymer, 0.06 wt% (1 mM) cyclo(RGDfC), 0.6 wt% (3.5 mM) VPM peptide, 20 mM HEPES pH 8.0; cell density per gel: 6,700.

MS substrate reactivity influences cell distribution within the hydrogel

For cell encapsulation, hydrogels were functionalized with cell-adhesive peptides and crosslinked with degradable peptide sequences followed reported protocols similar PEG gels.^{6a, 7,}

¹⁹ Keeping a general composition of (1:1) thiol:MS molar ratio, the cyclo(RGDfC) peptide was used to promote cell adhesion, and the VPM dithiol peptide was used as enzymatically-cleavable crosslinker. Hydrogels were prepared in HEPES pH 8.0 and mixed with cells.^{7, 19} Under these conditions, gelation time points ranged from 6 s (Ox), to 1.6 min (Tz) to 11.6 min (Bt). We imaged cell distribution within the hydrogels after encapsulation (Figure 4B). Cells encapsulated in Ox and Tz hydrogels appeared homogeneously distributed, while cells in Bt gels sedimented to some extent during the slower gelation process (ca. 40% of cells were found within the bottom 100 μm -layer of the gel). These results indicate that gelation time points from 6 s to a couple of minutes render gels with homogeneously distributed cells. Longer gelation times lead to sedimentation of the embedded cells. Note that under same conditions, thiol-Mal gels (gelation time point ca. 1 s) impeded proper homogenization of precursors and led to cell agglomeration at the upper part of the gel.⁷ In contrast, thiol-VS gels (gelation time point ca. 45 min) allowed proper homogenization of precursors but the slower gelation rate led to complete cell sedimentation during gelation.⁷ Taking together the results on the homogeneity of the gels at the microscale level (Fig. 4A) and at the cell distribution level (Fig. 4B), the Tz gel seems the most advantageous hydrogel candidate for cell encapsulation.

Optimization of aryl-thioether crosslinks to improve gel stability during cell culture

The cytocompatibility of the thiol-MS hydrogels was tested with L929 fibroblasts. The viability of the encapsulated cells after 1, 4, and 7 days of culture was quantified in live/dead assays. Cells remained viable (> 92%) in all hydrogels (**Figure 5A-B**), confirming the cytocompatibility of Ox gels⁷ and demonstrating the cytocompatibility of the novel Tz and Bt gels. The Ox gel was completely degraded by day 7, while Tz and Bt gels remained. The higher stability displayed by Tz and Bt gels versus Ox gels encouraged us to further investigate this aspect. Since the initial G' of the swollen hydrogels was similar for all cases (200-300 Pa, Figure S2C) and the concentration of VPM crosslinker was constant for all hydrogels, the different stability of the hydrogels was attributed to different stability of the aryl-thioether crosslinks in cell culture. Note that the stability of protein conjugates linked by aryl-thioether adduct was reported to decrease in the order Bt > Tz > Ox when incubated in human plasma (37°C, 72 h).^{8a} In such medium, the Ox-based aryl-thioether adduct cleaves into aryl-thiol and the exo-methylene β -eliminated product (Figure S4).^{8a}

Closer investigation of the stability profile of the different thiol-MS cell-laden gels under cell culture conditions (RPMI medium, pH 7.4, 37°C, 16 days) demonstrated the stability order: Tz > Bt > Ox (Figure 5C). Interestingly, the observed stability trend under cell culture does not follow the one previously reported in human plasma. However, enzymes secreted by cells during cell culture, in particular matrix-metalloproteinases (MMPs), might mediate different degradation mechanisms than proteins from human plasma. Overall, our results demonstrate that reactivity optimization of the heteroaryl MS substrate enables modulation of the degradation rate of derived thiol-MS gels under cell culture conditions. Remarkably, we found that cell-laden Tz gels are significantly more stable than Ox gels (15 vs 6 days, respectively), though less stable

than thiol-VS gels (> 16 days, Fig. S3). Nevertheless, the excellent performance of Tz gels regarding convenient gelation rate and high homogeneity makes this system a very good alternative for medium term cell culture experiments. Finally, the degradability rate of Tz gels could be further slowed down by use of other slowly degradable MMP-cleavable sequences such as GPQ peptides²⁰ as crosslinkers instead of VPM, to render more stable gels that enable longer term culture applications.

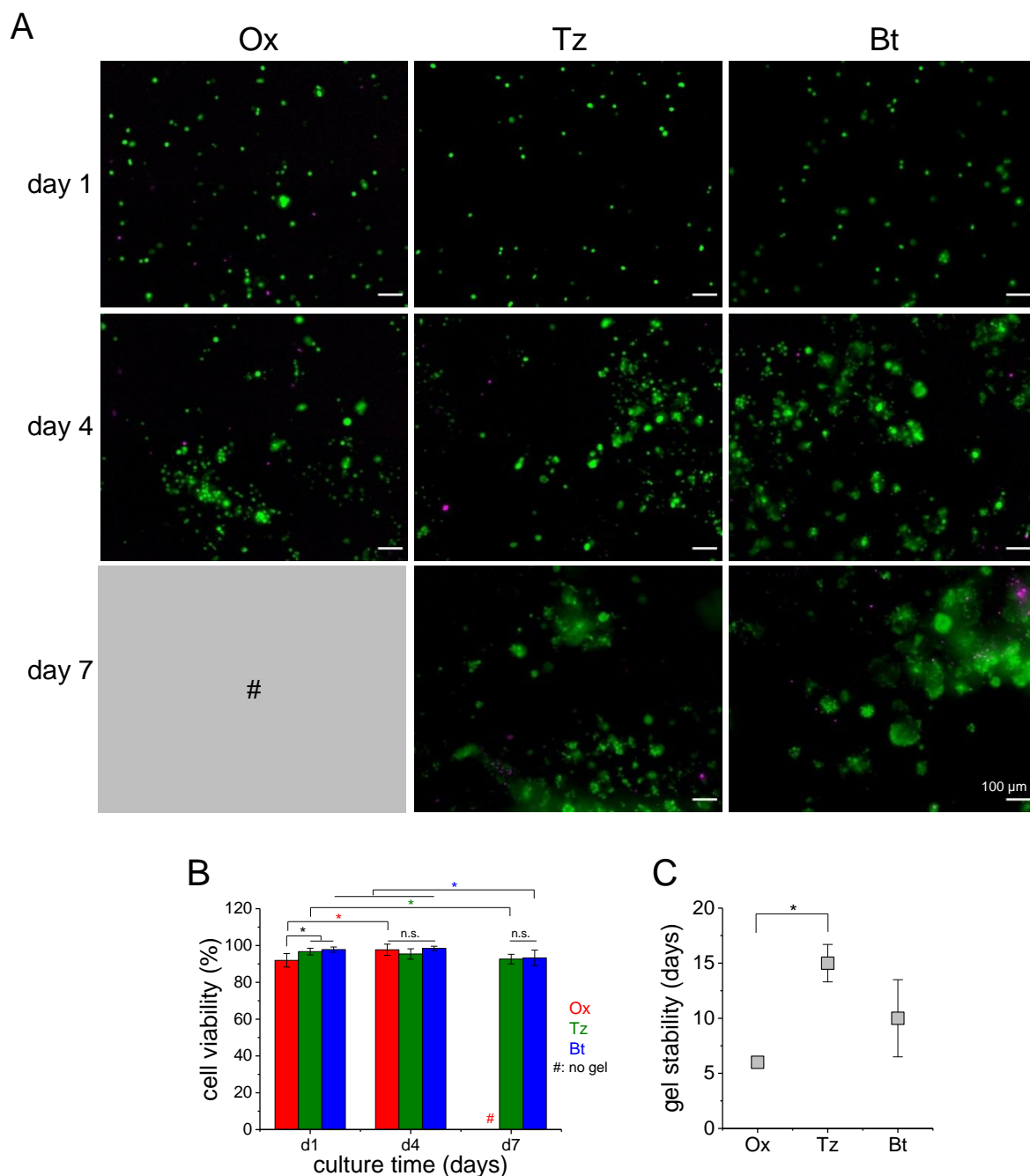


Figure 5. Encapsulation and culture of L929 fibroblasts in biofunctionalized thiol-MS gels. **A)** Fluorescence images and **B)** viability quantification, showing post-encapsulation survival at 1, 4 and 7 days. Live (green)/dead (magenta) assay was performed (scale bar = 100 μ m). **C)** Gel stability of the diverse thiol-MS systems under cell culture conditions. Gel composition: 5 wt% polymer, 0.07 wt% (1.3 mM) cyclo(RGDfC) and 0.7 wt % (4.3 mM) VPM, in 20 mM HEPES pH 8.0. Data are mean \pm SD (n= 3); *p<0.05, one-way ANOVA with Tukey post-hoc test; # means no gel.

3. Conclusions

In this work, two new PEG-MS precursors based on Tz and Bt MS substrates were developed and used for the fabrication of thiol-MS-based gels for cell encapsulation, and compared to the previously reported Ox variant. Intrinsic reactivity of the MS substrate decreased in the order Ox to Tz to Bt, resulting in materials with slower gelation rate and several benefits. We identified the novel Tz-based thiol-MS hydrogel as the most promising candidate for future biomedical applications. The higher synthetic accessibility, cost-efficiency, and good storage stability of Tz macromers should facilitate widespread use of derived materials. The Tz system maintains a tunable gelation kinetics (gelation times within seconds to hours), and allows comfortable cell manipulation and encapsulation. This gelation rate can be further adjusted over a wide range by external parameters such as pH and buffer concentration, and successfully exploited for stepwise crosslinking under physiological conditions. In relation to the previous thiol-MS design based on Ox analogue, Tz gels present higher microscale homogeneity and superior stability (15 days) for extended cell culture. These results highlight the importance of the molecular design of MS reactive precursors to render high performance biomaterials for cell encapsulation applications. Our findings expand the toolkit of thiol-mediated chemistries for synthesis of hydrogels with tailorable properties.

4. Experimental Section

Materials and methods

Chemicals and solvents had p.a. purity and were used as purchased unless otherwise noted. 4-arm (20 kDa) polyethyleneglycol (PEG) polymers end-functionalized with thiol (PEG-SH) and succinimidyl carboxymethyl ester (PEG-NHS) were purchased from Jenkem USA. PEG-MS precursors (i.e. PEG-Ox, PEG-Tz and PEG-Bt) were synthesized as follows. 4-arm (20 kDa) PEG-Ox macromer was synthesized according to our reported procedure.⁷ 4-arm (20 kDa) PEG-Tz and PEG-Bt macromers with high substitution degree (>90%) were synthesized according to the procedure described in the Supporting Information. Cyclo(RGDfC) and VPM peptide (GCRDVPMSMRGGDRCG) peptide sequences were acquired from Genecust (France); all other chemicals were purchased from Sigma Aldrich, Merck and Thermo Fischer Scientific (Germany). 20 mM HEPES buffer solutions were freshly prepared at pH 8.0; 7.5, 7.0 and 6.6, unless otherwise stated. PEG-MS and PEG-thiol precursor solutions were freshly prepared. After dissolving the macromers in the corresponding buffer, the solutions were vortex-mixed, ultrasonicated (ca 5 s) and centrifuged to eliminate bubbles. The final pH of the precursor solutions was verified with a pH-meter (pH-1 micro, Presens, DE).

Estimation of gelation time of hydrogels by the macroscopic “pipetting” test

A macroscopic test was used to estimate the gelation time of hydrogels.⁷ Precursors solutions at a given concentration and pH were prepared as detailed above. 30 μ L of PEG-MS precursor solution was placed in a plastic Eppendorf vial, followed by addition of 30 μ L of PEG-thiol precursor solution and a stopwatch was started. The curing solution was continuously mixed with pipette (size of pipette tip= 2-200 μ L, 53 mm; from Eppendorf epT.I.P.S.®, Germany) until the

gelling solution stopped flowing. Time was measured using a Rotilabo-Signal-Timer TR 118 (Roth, Germany) stopwatch. Gelation time was taken as the time elapsed between the mixing of the two components and the moment when pipetting of the mixture was no longer possible.

Rheology of hydrogels during in situ crosslinking (before swelling)

The rheological properties of hydrogels were measured on a Discovery HR-3 rheometer (TA Instruments, USA) using 12 mm parallel plates and a Peltier stage temperature control system. Precursor solutions were prepared as above. 20 μ L of PEG-MS solution was loaded on the rheometer's Peltier lower plate, followed by addition of 20 μ L of PEG-thiol solution and mixing with pipette tip directly on the plate. The upper plate was approached to reach a gap size of 300 μ m and the sample was sealed with paraffin or silicon oil to avoid evaporation during measurement, unless otherwise stated. The total time required for sample loading and start of measurement was approximately 60 s. Strain sweeps (0.1 to 1000% strain at frequency = 1 Hz) and frequency sweeps (0.01 to 100 Hz at strain = 1%) were performed to determine the linear viscoelastic regime. Time sweep measurements were carried out within such regime using the following parameters: starting gap of 300 μ m, controlled axial force (0.0 ± 0.1 N), frequency 1 Hz, strain 1%, temperature = 25°C, unless otherwise stated. Gelation time point was estimated from the time sweep curves as the time at which $G' = G''$.

Time sweep measurement during stepwise curing of Tz-derived thiol-MS gels

Tz gels were prepared at 5 wt% concentration in 10 mM HEPES pH 7.0 for in situ measurement as above stated. The curing sample was set on the rheometer plate and allowed to cure in air for 20 min. At this time point, the curing sample was swollen in situ by injecting a

buffer of given pH (7.0 or 8.0) and concentration (10-50 mM) around, while the gelation continued until a total time of 2 h. Evolution of G' at the different gelation steps was followed.

Rheology of hydrogels after swelling

25 μL of PEG-MS solution was placed in a PDMS cylindrical mold (8 mm diameter), quickly mixed with 25 μL of PEG-thiol solution, and allowed to crosslink in a humid chamber at room temperature for 2 h. The obtained gels were carefully demolded and swollen for 24 h in 20 mM HEPES at the corresponding pH value. Swollen hydrogels (ca 9-10 mm diameter) were loaded to the rheometer and measured using upper plate geometry of 8 mm diameter with rough surface to ensure a good contact with the swollen gel. Time sweep measurements were carried out for 3 min to avoid sample's evaporation, using the following parameters: starting controlled axial force 0.05 N, variable starting gap (depending on sample's thickness, typically 700-1000 μm), frequency 1 Hz, strain 1%, temperature = 25°C.

Statistical analysis. Data were expressed as mean \pm standard deviation (SD). For each condition, typically 3 independent rheology experiments were performed. A one-way analysis of variance (ANOVA) with a Tukey test of the variance was used to determine the statistical significance between groups. The statistical analysis was performed to compare different groups and significant difference was set to $*p < 0.05$.

Determination of mass swelling ratio of hydrogels

Hydrogels with initial volume of 100 μL were prepared in a PDMS mold at pH 7.5 and swollen in water for 24 h. The mass of the swollen gel (M_s) was measured by gravimetry. The gels were dried in an oven at 37°C until a constant weight (typically 48 h). The mass of the dry

gel was measured (M_d). The mass swelling ratio (SR) was calculated with equation 1. Experiments were performed in triplicate. Mean and standard deviation values are presented.

$$SR = \frac{M_s - M_d}{M_d} \quad (\text{equation 1})$$

Stability study of acellular hydrogels in cell culture medium

Hydrogels with initial volume of 100 μ L were prepared in a PDMS mold at pH 7.5 and swollen in HEPES buffer pH 7.5 (\sim 3 mL) for 24 h at 37°C. The swelling medium was changed to RPMI cell culture medium containing 10% fetal bovine serum proteins (FBS) and 1% penicillin/streptomycin (PS) (\sim 5 mL) (denoted as RPMI+). The gels were allowed to swell for 24 h at 37°C. This was considered the starting point of the study ($t=0$) and the mass of the swollen gel was measured gravimetrically. Incubation of gels in RPMI+ continued at 37°C for increasing time until 3 weeks. At selected time points (typically, 1-2 times per week) the swollen gel was removed from the incubating solution, the excess of liquid was blotted using Kimberly-Clark Professional precision wipes and the mass of the swollen gel was measured. The medium was changed by fresh one after every determination and gels were placed in a new cell culture plate every week. The gel's stability was followed by plotting the normalized mass of the swollen gel at increasing incubation times. Normalized mass of swollen gel upon incubation in medium was calculated according to equation 2. Experiments were performed in triplicate. Mean and standard deviation values are presented.

$$\text{normalized mass of swollen gel} = \frac{M_t}{M_i} \quad (\text{equation 2})$$

Fluorescence imaging of hydrogels and study of microscale homogeneity

An adapted protocol was followed.¹⁵ All solutions were prepared in 20 mM HEPES buffer pH 8.0. 5 wt% PEG-thiol solution (43.2 μ L) was fluorescently labeled by incubating 0.5 mM Alexa Fluor 350 C5-maleimide (A30505, Life Technologies) (1.8 μ L) for 15 min at 37 °C. Then, 5 wt% PEG-MS (5 μ L) was spotted in a plastic μ -slide angiogenesis (Ibidi, DE) followed by addition of labeled PEG-thiol solution (5 μ L) to the same well and mixing of the precursors. The mixture was cured for 15 min at 37 °C and HEPES buffer was added to the well. Final gel composition was 5 wt% polymer and 0.01 mM fluorophore. Gels were imaged with Zeiss LSM 880 confocal microscope with a 10X air objective. Imaging was performed in the tiles mode (5x5 images with 10% overlap), in the center of the gel with respect to the z-direction. Image analysis was performed using Image J (NIH) and ZEN (black edition). In order to investigate the homogeneity of formed gels, profile plots of dye labeled gels were drawn in ZEN (black edition) (plot profile command) with a cross-section of interest for at least three different gel samples, giving pixel intensity across the gel distance. For visualization and readability purposes, the brightness of images was adjusted when needed. For data treatment, raw images (gray values of intensity) were used.

Cell culture protocol

Fibroblast L929 cell line (ATCC) was cultured at 37 °C and 5% CO₂ in RPMI 1640 medium (Gibco, 61870-010) supplemented with 10% FBS (Gibco, 10270) and 1% P/S (Invitrogen) as established in the literature.²¹ For the encapsulation experiments, L929 cells (1×10^6 mL⁻¹ cells) were counted and resuspended in medium to achieve a final cell density of 27,000 cells per gel, unless otherwise stated.^{6a, 22}

Hydrogel preparation for 3D cell culture

PEG hydrogels were prepared by adapting previously reported protocols.^{6a, 19} Precursor solutions of PEG-MS (100 mg mL⁻¹, 10 wt%, 20 mM MS groups) were prepared by dissolving the lyophilized polymer in sterile HEPES buffer (20 mM, pH 8.0) inside a sterile laminar flow and used directly without further filtration. Solution of cyclo(RGDfC) (2.9 mg mL⁻¹, 5 mM) was prepared in sterile HEPES buffer (20 mM, pH 8.0), while solution of VPM peptide (GCRDVPMSMRGGDRCG, 36.8 mg mL⁻¹, 21.7 mM) was prepared in sterile HEPES buffer (20 mM, pH 8.0) that contained 1.5 mM NaHCO₃. PEG-MS stock solution (46 µL, 10 wt%) was mixed with cyclo(RGDfC) (24 µL, 5 mM) and incubated for 30 min at 37 °C. The fibroblast cell pellet (3 µL) was resuspended in the above solution (3.6x10⁵ cells mL⁻¹, cell density within the typical range of 3x10⁵ - 3x10⁷ cells mL⁻¹ as reported in published work^{6a, 19, 22-23}) and 8 µL of resulting mixture were placed in an Ibidi 15-µwell angiogenesis slide. Immediately, the solution of VPM peptide (2 µL, 21.7 mM) was added to the µ-well, carefully mixed with pipette tip and allowed to crosslink. Ox and Tz-based hydrogels were let to polymerize for 30 min, while Bt-based hydrogels were let to polymerize for 45 min at 37 °C and 5% CO₂. After gelation, RPMI medium was added and culture was maintained for 1, 4 and 7 days. Medium (45 µL) was added to each well and substituted by fresh medium every 24 h during cell culture. Final gel composition was 5 wt% polymer, 0.07 wt% (1.3 mM) cyclo(RGDfC) and 0.7 wt % (4.3 mM) VPM.

Quantification of cell distribution across gels

Experiments were performed in triplicates. In this case, final gel composition was 4 wt% polymer, 0.06 wt% (1 mM) cyclo(RGDfC) and 0.6 wt % (3.5 mM) VPM; and L929 fibroblasts

were encapsulated in thiol-MS hydrogels at 6,700 cells per gel (to have a lower density for visualization). After 1 h post-encapsulation, cell culture medium was removed. Samples were incubated in DAPI solution (1:5000 in PBS) for nuclear labeling (1 h at room temperature). Samples were washed 4 times with PBS for 10 min, and imaged with Zeiss LSM 880 confocal microscope with a 10X air objective, using Z-stack mode and 50 μm per stack. The number of cells per stack was counted.

Live/dead Assay

L929 fibroblasts were cultured in thiol-MS PEG hydrogels for 1-7 days and cell culture medium was removed. Samples were incubated for 5 min with fluorescein diacetate (40 $\mu\text{g mL}^{-1}$) and propidium iodide (30 $\mu\text{g mL}^{-1}$) in PBS, washed twice with PBS and imaged with Zeiss Axio Observer microscope. For each sample, at least 5 independent z-stacks at 20x magnification were analyzed (~1200-1400 cells per sample). Live and dead cells were counted manually in each slice (50 μm) of z-stack to calculate the percentage viability of each sample.

Statistical analysis. All experiments comprised of at least 3 independent experimental batches. Data are expressed as mean \pm SD. A one-way analysis of variance (ANOVA) with a Tukey test of the variance was used to determine the statistical significance between groups. The statistical analysis was performed to compare different groups and significant difference was set to $*p < 0.05$.

ASSOCIATED CONTENT

Supporting Information. Supporting Information containing the synthesis of intermediates and final macromers, additional results on rheological characterization and supplementary cell

studies.

AUTHOR INFORMATION

Corresponding Authors

* Dr. Julieta I. Paez: julieta.paez@leibniz-inm.de; ORCID ID: 0000-0001-9510-7254.

* Prof. Dr. Aránzazu del Campo: aranzazu.delcampo@leibniz-inm.de , ORCID ID: 0000-0001-5725-2135.

Author Contributions

The manuscript was written through contributions of all authors. All authors have given approval to the final version of the manuscript.

Funding Sources

J.I.P. and M.J. received funding from the Deutsche Forschungsgemeinschaft (DFG, Project no. 422041745). A.R. received funding from the Deutscher Akademischer Austauschdienst (DAAD, Exchange Internship Program). R.V.M, S.P. and A.d.C received funding from the European Union's Horizon 2020 research and innovation programme under the FET PROACTIVE grant agreement no. 731957 (Mechano-Control).

ACKNOWLEDGMENTS

We thank Josef Zapp (Saarland University) for help with 500-MHz NMR measurements, Klaus Hollemeyer (Saarland University), Claudia Fink-Straube and Ha Rimbach-Nguyen (INM) for

mass spectrometry measurements, Prof. Markus Gallei and Blandine Boßmann (Saarland University) for GPC measurements, and Britta Abt (INM) for providing cells for the encapsulation experiments.

References

1. (a) Tibbitt, M. W.; Anseth, K. S., Hydrogels as extracellular matrix mimics for 3D cell culture. *Biotechnology and Bioengineering* **2009**, *103* (4), 655-663; (b) Magno, V.; Meinhardt, A.; Werner, C., Polymer Hydrogels to Guide Organotypic and Organoid Cultures. *Adv. Funct. Mater.* **2020**, *30* (48), 2000097.
2. Durst, C. A.; Cuchiara, M. P.; Mansfield, E. G.; West, J. L.; Grande-Allen, K. J., Flexural characterization of cell encapsulated PEGDA hydrogels with applications for tissue engineered heart valves. *Acta Biomater.* **2011**, *7* (6), 2467-2476.
3. Qin, X.-H.; Wang, X.; Rottmar, M.; Nelson, B. J.; Maniura-Weber, K., Near-Infrared Light-Sensitive Polyvinyl Alcohol Hydrogel Photoresist for Spatiotemporal Control of Cell-Instructive 3D Microenvironments. *Adv. Mater.* **2018**, *30* (10), 1705564.
4. (a) Ma, Y.-H.; Yang, J.; Li, B.; Jiang, Y.-W.; Lu, X.; Chen, Z., Biodegradable and injectable polymer–liposome hydrogel: a promising cell carrier. *Polym. Chem.* **2016**, *7* (11), 2037-2044; (b) McKinnon, D. D.; Domaille, D. W.; Cha, J. N.; Anseth, K. S., Biophysically Defined and Cytocompatible Covalently Adaptable Networks as Viscoelastic 3D Cell Culture Systems. *Adv. Mater.* **2014**, *26* (6), 865-872; (c) Grover, G. N.; Lam, J.; Nguyen, T. H.; Segura, T.; Maynard, H. D., Biocompatible Hydrogels by Oxime Click Chemistry. *Biomacromolecules* **2012**, *13* (10), 3013-3017.
5. (a) DeForest, C. A.; Polizzotti, B. D.; Anseth, K. S., Sequential click reactions for synthesizing and patterning three-dimensional cell microenvironments. *Nat. Mater.* **2009**, *8*, 659-664; (b) Smith, L. J.; Taimoory, S. M.; Tam, R. Y.; Baker, A. E. G.; Binte Mohammad, N.; Trant, J. F.; Shoichet, M. S., Diels–Alder Click-Cross-Linked Hydrogels with Increased Reactivity Enable 3D Cell Encapsulation. *Biomacromolecules* **2018**, *19* (3), 926-935; (c) Alge, D. L.; Azagarsamy, M. A.; Donohue, D. F.; Anseth, K. S., Synthetically Tractable Click Hydrogels for Three-Dimensional Cell Culture Formed Using Tetrazine–Norbornene Chemistry. *Biomacromolecules* **2013**, *14* (4), 949-953.
6. (a) Phelps, E. A.; Enemchukwu, N. O.; Fiore, V. F.; Sy, J. C.; Murthy, N.; Sulchek, T. A.; Barker, T. H.; García, A. J., Maleimide cross-linked bioactive PEG hydrogel exhibits improved reaction kinetics and cross-linking for cell encapsulation and in situ delivery. *Adv. Mater.* **2012**, *24* (1), 64-70; (b) Pupkaite, J.; Rosenquist, J.; Hilborn, J.; Samanta, A., Injectable Shape-Holding Collagen Hydrogel for Cell Encapsulation and Delivery Cross-linked Using Thiol-Michael Addition Click Reaction. *Biomacromolecules* **2019**, *20* (9), 3475-3484; (c) Lutolf, M. P.; Raeber, G. P.; Zisch, A. H.; Tirelli, N.; Hubbell, J. A., Cell-responsive synthetic hydrogels. *Adv. Mater.* **2003**, *15* (11), 888-892.

7. Paez, J. I.; Farrukh, A.; Valbuena-Mendoza, R.; Włodarczyk-Biegun, M. K.; del Campo, A., Thiol-Methylsulfone-Based Hydrogels for 3D Cell Encapsulation. *ACS Appl. Mater. Interfaces* **2020**, *12* (7), 8062-8072.
8. (a) Toda, N.; Asano, S.; Barbas, C. F., Rapid, Stable, Chemoselective Labeling of Thiols with Julia–Kocięński-like Reagents: A Serum–Stable Alternative to Maleimide–Based Protein Conjugation. *Angew. Chem., Int. Ed.* **2013**, *52* (48), 12592-12596; (b) Chen, X.; Wu, H.; Park, C.-M.; Poole, T. H.; Keceli, G.; Devarie-Baez, N. O.; Tsang, A. W.; Lowther, W. T.; Poole, L. B.; King, S. B.; Xian, M.; Furdui, C. M., Discovery of Heteroaromatic Sulfones As a New Class of Biologically Compatible Thiol-Selective Reagents. *ACS Chem. Biol.* **2017**, *12* (8), 2201-2208.
9. (a) Farrukh, A.; Paez, J. I.; Salierno, M.; del Campo, A., Bioconjugating thiols to poly(acrylamide) gels for cell culture using methylsulfonyl co-monomers. *Angew. Chem. Int. Ed.* **2016**, *55* (6), 2092-2096; (b) Motiwala, H. F.; Kuo, Y.-H.; Stinger, B. L.; Palfey, B. A.; Martin, B. R., Tunable Heteroaromatic Sulfones Enhance in-Cell Cysteine Profiling. *J. Am. Chem. Soc.* **2020**, *142* (4), 1801-1810.
10. Patenaude, M.; Campbell, S.; Kinio, D.; Hoare, T., Tuning gelation time and morphology of injectable hydrogels using Ketone-Hydrazide cross-linking. *Biomacromolecules* **2014**, *15* (3), 781-790.
11. Terrier, F., *Modern Nucleophilic Aromatic Substitution*. 2013; p 1-472.
12. Campodónico, P. R., Solvent Effect on a Model of S_NAr Reaction in Conventional and Non-Conventional Solvents. In *Solvents, Ionic Liquids and Solvent Effects*, Glossman-Mitnik, D.; Maciejewska, M., Eds. IntechOpen: Rijeka, 2020.
13. (a) Yoshitake, M.; Kamiyama, Y.; Nishi, K.; Yoshimoto, N.; Morita, M.; Sakai, T.; Fujii, K., Defect-free network formation and swelling behavior in ionic liquid-based electrolytes of tetra-arm polymers synthesized using a Michael addition reaction. *Physical Chemistry Chemical Physics* **2017**, *19* (44), 29984-29990; (b) Tang, J.; Katashima, T.; Li, X.; Mitsukami, Y.; Yokoyama, Y.; Sakumichi, N.; Chung, U.-i.; Shibayama, M.; Sakai, T., Swelling Behaviors of Hydrogels with Alternating Neutral/Highly Charged Sequences. *Macromolecules* **2020**, *53* (19), 8244-8254.
14. Rutz, A. L.; Hyland, K. E.; Jakus, A. E.; Burghardt, W. R.; Shah, R. N., A Multimaterial Bioink Method for 3D Printing Tunable, Cell-Compatible Hydrogels. *Adv. Mater.* **2015**, *27* (9), 1607-1614.
15. Darling, N. J.; Hung, Y. S.; Sharma, S.; Segura, T., Controlling the kinetics of thiol-maleimide Michael-type addition gelation kinetics for the generation of homogenous poly(ethylene glycol) hydrogels. *Biomaterials* **2016**, *101*, 199-206.
16. Haines-Butterick, L.; Rajagopal, K.; Branco, M.; Salick, D.; Rughani, R.; Pilarz, M.; Lamm, M. S.; Pochan, D. J.; Schneider, J. P., Controlling hydrogelation kinetics by peptide design for three-dimensional encapsulation and injectable delivery of cells. *Proceedings of the National Academy of Sciences* **2007**, *104* (19), 7791-7796.
17. Schultz, K. M.; Kyburz, K. A.; Anseth, K. S., Measuring dynamic cell–material interactions and remodeling during 3D human mesenchymal stem cell migration in hydrogels. *Proceedings of the National Academy of Sciences* **2015**, *112* (29), E3757-E3764.
18. (a) Worthington, P.; Drake, K. M.; Li, Z.; Napper, A. D.; Pochan, D. J.; Langhans, S. A., Implementation of a High-Throughput Pilot Screen in Peptide Hydrogel-Based Three-Dimensional Cell Cultures. *SLAS DISCOVERY: Advancing the Science of Drug Discovery* **2019**, *24* (7), 714-723; (b) Rimann, M.; Angres, B.; Patocchi-Tenzer, I.; Braum, S.; Graf-Hausner, U.,

Automation of 3D Cell Culture Using Chemically Defined Hydrogels. *Journal of Laboratory Automation* **2014**, *19* (2), 191-197.

19. Farrukh, A.; Paez, J. I.; del Campo, A., 4D Biomaterials for Light-Guided Angiogenesis. *Adv. Funct. Mater.* **2019**, *29* (6), 1807734.

20. (a) Patterson, J.; Hubbell, J. A., Enhanced proteolytic degradation of molecularly engineered PEG hydrogels in response to MMP-1 and MMP-2. *Biomaterials* **2010**, *31* (30), 7836-7845; (b) Fairbanks, B. D.; Schwartz, M. P.; Halevi, A. E.; Nuttelman, C. R.; Bowman, C. N.; Anseth, K. S., A Versatile Synthetic Extracellular Matrix Mimic via Thiol-Norbornene Photopolymerization. *Adv. Mater.* **2009**, *21* (48), 5005-5010.

21. Takeuchi, A.; Hayashi, H.; Naito, Y.; Baba, T.; Tamatani, T.; Onozaki, K., Human Myelomonocytic Cell Line THP-1 Produces a Novel Growth-promoting Factor with a Wide Target Cell Spectrum. *Cancer Res.* **1993**, *53* (8), 1871-1876.

22. Lee, S.-H.; Moon, J. J.; West, J. L., Three-dimensional micropatterning of bioactive hydrogels via two-photon laser scanning photolithography for guided 3D cell migration. *Biomaterials* **2008**, *29* (20), 2962-2968.

23. (a) Bott, K.; Upton, Z.; Schrobback, K.; Ehrbar, M.; Hubbell, J. A.; Lutolf, M. P.; Rizzi, S. C., The effect of matrix characteristics on fibroblast proliferation in 3D gels. *Biomaterials* **2010**, *31* (32), 8454-8464; (b) Moon, J. J.; Saik, J. E.; Poché, R. A.; Leslie-Barbick, J. E.; Lee, S.-H.; Smith, A. A.; Dickinson, M. E.; West, J. L., Biomimetic hydrogels with pro-angiogenic properties. *Biomaterials* **2010**, *31* (14), 3840-3847; (c) Adelöw, C.; Segura, T.; Hubbell, J. A.; Frey, P., The effect of enzymatically degradable poly(ethylene glycol) hydrogels on smooth muscle cell phenotype. *Biomaterials* **2008**, *29* (3), 314-326; (d) DeForest, C. A.; Anseth, K. S., Cytocompatible click-based hydrogels with dynamically tunable properties through orthogonal photoconjugation and photocleavage reactions. *Nat. Chem.* **2011**, *3*, 925-931.